DFT, FT-Raman, FTIR, NMR, and UV–Vis Studies of a Hetarylazo Indole Dye

Berna Çatıkkaş,*[a] Ebru Aktan,[b] and Zeynel Seferoğlu[b]

In this study, computational calculations of 1,2-dimethyl-3-[(5-methylsulfanyl-1,3,4-thiadiazol-2-yl)diazenyl]-1H-indole have been carried out using the Becke-3-Lee–Yang–Parr density functional methods with 6-311+G(d,p) basis set. The geometry optimization and fundamental frequencies of the most stable configuration have been calculated. The FTIR and FT-Raman spectra of the compound have been recorded and compared to the calculated frequency values. The total energy distribution of the fundamental modes has been obtained using scaled quantum mechanical program. The ^{1}H NMR chemical shifts have been calculated using the gauge-independent atomic orbital approach. The theoretical electronic absorption spectra have been calculated using time-dependent density functional theory. The conductor-like screening solvation model has been applied to calculate the chemical shifts and maximum absorption wavelength values. The calculated values have been compared with the corresponding experimental results.
© 2012 Wiley Periodicals, Inc.

DOI: 10.1002/qua.24043

Introduction

Azo compounds, with two phenyl or hetaryl rings separated by an azo (N=N) bond, have been used as dyes and pigments for a long time in research areas both fundamental and applied.[1] It is well known that the azo compounds are the most widely used class of dyes, because of their versatile application in various fields such as dyeing of textile fibers, coloring of different materials, and biological–medicinal studies. They are also used as acid–base, redox, and metallochromic indicator[2–12] in the fields of nonlinear optics, optical data storage, advanced applications in organic synthesis, and analytical chemistry. Their optical properties depend not only on the spectroscopic properties of the molecules but also on their crystallographic arrangements.[13,14] To the best of our knowledge, the crystal and molecular structures of several monoazo disperse dyes, including azoindole derivatives have been reported only in Ref. [15–18]. We have also synthesized the 1,2-dimethyl-3-[(5-methylsulfanyl-1,3,4-thiadiazol-2-yl)diazenyl]-1H-indole (DMIA) molecule.[18]

The aim of this work is to predict the structural, electronic, and vibrational spectral parameters of the title compound. To use the change of the vibration spectra as a probe for understanding the DMPI target interactions, the structural and vibrational properties should be fully known. DMIA molecule is shown in Figure 1. In addition, to facilitate the assignment, density functional theory (DFT) vibration studies should are also incorporated.

Experimental Details

The infrared spectrum of DMIA was recorded in the middle-infrared 4000–400 cm^{-1} region and the far-infrared 400–20 cm^{-1} one by a Bruker FTIR IFS 66v/S spectrometer and the assignments of the observed bands were made with 0.2 cm^{-1} resolution. The samples were prepared as mulls in Nujol and as a KBr disc, which was calibrated using polystyrene bands. The FT-Raman spectrum was obtained on a Bruker Senterra Dispersive Raman Microscope using the 735 nm excitation.

Results and Discussion

Structural parameters

For the ground-state geometry, the conformation analysis of the molecule was investigated theoretically by performing a DFT calculation. The potential energy surface (PES) scan for torsion angles (N_{10}—N_{11}—C_{25}—C_{28}) and (N_{28}—C_{24}—C_{29}—C_{30}) was carried out at 10○ intervals in the range 0–360○ at the Hartree–Fock level, with the 6-31G(d) basis set. The results from the PES scan were reoptimized at the DFT level, using the Becke3-Lee-Yang-Parr hybrid functional (B3LYP)[19] with 6-311+G(d,p) basis set. Four stable conformers and their energies are shown in Figure 2. The geometries were fully optimized with tight convergence criteria. These structures were local minima on the PES.

The relative abundances N_i (the population of the different conformers) of the possible conformers found were calculated using the Boltzmann distribution:

$$\frac{N_i}{N_j} = \frac{g_i}{g_j} exp\left[\frac{-(E_i - E_j)}{RT}\right],$$

where the subscripts i and j represent the highest and lowest energies and g is the degeneracy ($N_1 + N_2 + N_3 + N_4 = 1$).

[a] B. Çatıkkaş
Department of Physics, Mustafa Kemal University, 31034, Hatay, Türkiye
Fax: (+90) 326 2455867
E-mail: agberna@yahoo.com
[b] E. Aktan, Z. Seferoğlu
Department of Chemistry, Gazi University, 06500, Ankara, Türkiye

© 2012 Wiley Periodicals, Inc.

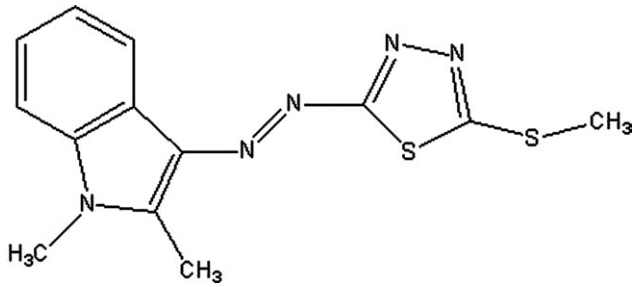


Figure 1. The DMIA molecule.

The calculated population percentages of the conformers for the title molecule by the above equation are shown in Table 1.

The most stable conformation of DMIA we found is molecule **1** (gas phase) which does not coincided with the conformation in the crystalline structure **2.** This difference is likely due to the molecular packing effects in the crystal form. All conformations (**1**, **2**, **3**, and **4**) are shown in the Figure 2. The most stable conformation with the numbering of atoms is shown in Figure 3.

One can conclude that our calculation is successful, as the difference between calculated and experimental bond lengths is at most about 0.01–0.02 Å. That difference for the bond and torsion angles is at most about 1–2°. These values satisfy the reliability criterion of the calculated structural parameters, developed by Foresman and Frisch.[20] The selected bond lengths (*R*), bond angles (*A*), and dihedral angles (*D*) for the dye, determined by X-ray diffraction,[21] B3LYP/6-311+G(d,p) are listed in Table 2.

Table 1. The calculated population percentages of the conformers.

Conformers	Total energy (a.u.)	Percentage (%)
1	−1573.54466686	98.72
2	−1573.54052553	1.23
3	−1573.53749822	5.02×10^{-6}
4	−1573.53367123	8.74×10^{-8}

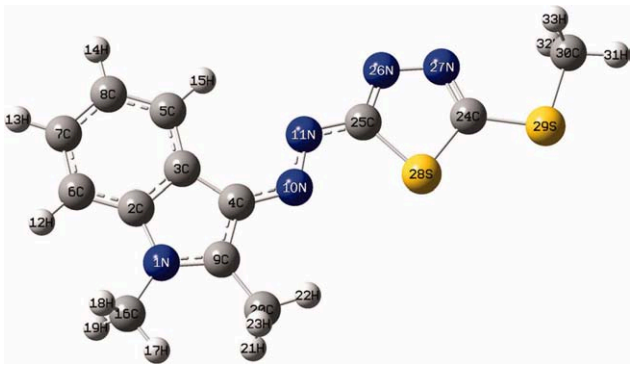


Figure 3. The structure and atom numbering of the most stable conformation of DMIA molecule (**1**). [Color figure can be viewed in the online issue, which is available at wileyonlinelibrary.com.]

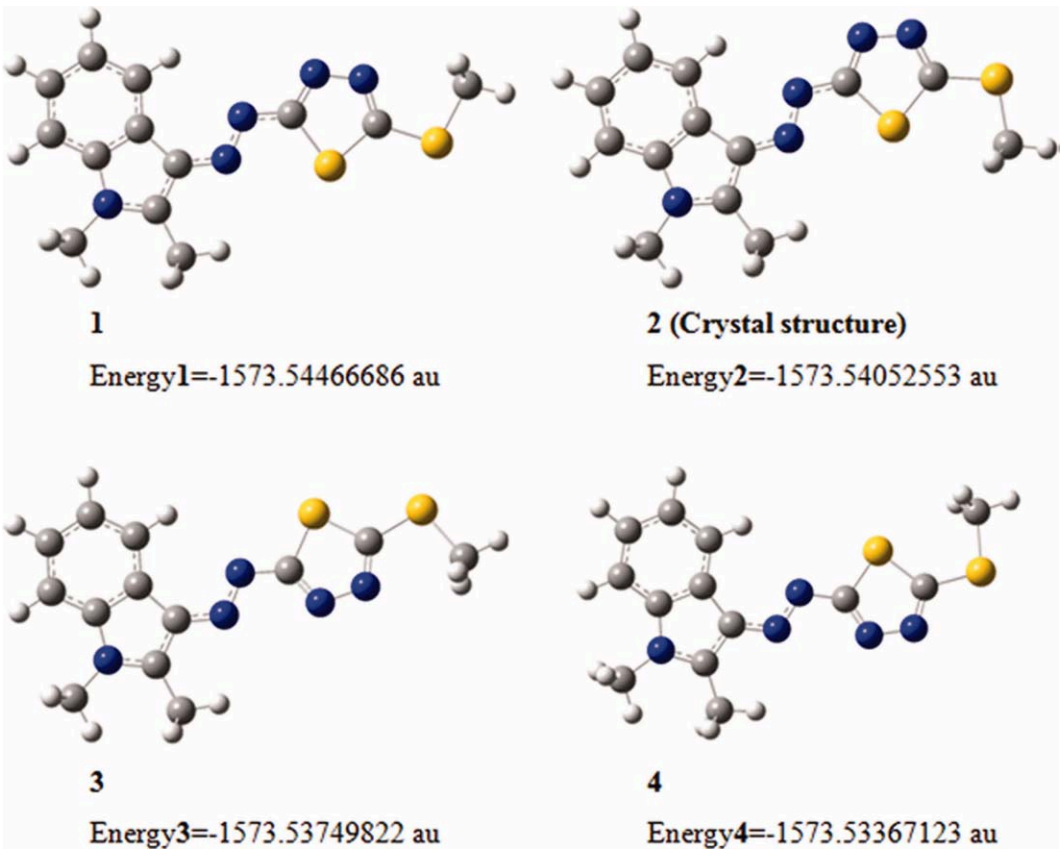


Figure 2. Four different conformers of the DMIA molecule. [Color figure can be viewed in the online issue, which is available at wileyonlinelibrary.com.]

1097461x, 2013, 5, Downloaded from https://onlinelibrary.wiley.com/doi/10.1002/qua.24043 by T.C. Cumhurbaskanligi Kutuphanesi, Wiley Online Library on [20/02/2025]. See the Terms and Conditions (https://onlinelibrary.wiley.com/terms-and-conditions) on Wiley Online Library for rules of use; OA articles are governed by the applicable Creative Commons License

Table 2. The selected calculated and experimental geometric parameters for the most stable conformation of the DMIA.

R	Calc.	Exp.*	*A*	Calc.	Exp.*	*D*	Calc.	Exp.*
(1–2)	1.399	1.392(3)	(2–1–9)	109.4	109.9(2)	(9–1–2–3)	0.0	0.1(3)
(1–9)	1.366	1.356(4)	(2–1–16)	123.6	123.8(3)	(9–1–2–6)	180.0	178.3 (3)
(1–16)	1.453	1.467(4)	(9–1–16)	126.9	126.2(3)	(16–1–2–3)	180.0	177.6(3)
(2–3)	1.413	1.407(4)	(1–2–3)	108.4	108.2(2)	(16–1–2–6)	0.0	3.9(5)
(2–6)	1.392	1.387(4)	(1–2–6)	129.1	129.3(3)	(2–1–9–4)	0.0	0.8(3)
(3–4)	1.450	1.439(4)	(3–2–6)	122.5	122.5(3)	(2–1–9–20)	180.0	178.1(3)
(3–5)	1.400	1.396(4)	(2–3–4)	105.8	105.8(2)	(16–1–9–4)	180.0	176.9(3)
(4–9)	1.401	1.400(4)	(2–3–5)	119.3	118.7(3)	(16–1–9–20)	0.0	4.2(5)
(4–10)	1.364	1.357(4)	(4–3–5)	135.0	135.5(3)	(1–2–3–4)	0.0	0.6(3)
(5–8)	1.392	1.386(4)	(3–4–9)	107.6	107.8(2)	(1–2–3–5)	180.0	176.9(2)
(5–15)	1.081	0.93	(3–4–10)	132.0	133.0(3)	(6–2–3–4)	180.0	179.2(3)
(6–7)	1.393	1.373(4)	(9–4–10)	120.4	119.1(3)	(6–2–3–5)	0.0	1.7(4)
(6–12)	1.084	0.93	(3–5–8)	118.5	118.2(3)	(3–2–6–7)	0.0	2.0(4)
(7–8)	1.403	1.386(4)	(2–6–7)	117.2	117.9(3)	(2–3–4–9)	0.0	1.1(3)
(7–13)	1.084	0.93	(5–8–7)	121.4	122.3 (3)	(2–3–4–10)	180.0	177.7(3)
(8–14)	1.084	0.93	(1–9–4)	108.8	108.3(2)	(5–3–4–9)	180.0	175.8(3)
(9–20)	1.489	1.478(4)	(1–9–20)	123.6	123.2(3)	(5–3–4–10)	0.0	5.4(6)
(10–11)	1.273	1.299(3)	(4–10–11)	116.1	115.3(2)	(2–3–5–8)	0.0	0.2(4)
(11–25)	1.376	1.388(4)	(10–11–25)	113.6	110.4(2)	(4–3–5–8)	180.0	176.3(3)
(16–17)	1.088	0.96	(20–9–4)	127.7	128.5(3)	(3–4–9–1)	0.0	1.2(3)
(16–18)	1.093	0.96	(27–24–28)	114.9	115.2(2)	(3–4–9–20)	180.0	177.7(3)
(16–19)	1.093	0.96	(27–24–29)	124.3	119.3(2)	(10–4–9–20)	0.0	3.3(5)
(20–21)	1.095	0.96	(28–24–29)	120.8	125.4(18)	(3–4–10–11)	0.0	2.7(5)
(20–22)	1.089	0.96	(11–25–26)	122.3	120.5(3)	(9–4–10–11)	180.0	176.0(2)
(20–23)	1.095	0.96	(25–26–27)	113.4	111.2(3)	(3–5–8–7)	0.0	1.8(5)
(24–27)	1.306	1.296(4)	(24–27–26)	113.0	112.4(2)	(4–10–11–25)	180.0	179.8(2)
(24–28)	1.753	1.728(3)	(24–28–25)	85.0	85.78(15)	(10–11–25–26)	180.0	178.3(3)
(24–29)	1.755	1.736(3)	(24–29–30)	100.1	102.90(15)	(10–11–25–28)	0.0	0.5(4)
(25–26)	1.302	1.305(4)				(28–24–27–26)	0.0	0.5(4)
(25–28)	1.786	1.730(3)				(29–24–27–26)	180.0	176.6(2)
(26–27)	1.363	1.388(3)				(27–24–28–25)	0.0	0.2(3)
(29–30)	1.827	1.785(3)				(29–24–28–25)	180.0	176.8(2)
						(27–24–29–30)	0.0	172.8 (3)
						(28–24–29–30)	180.0	10.3 (3)
						(11–25–26–27)	180.0	179.5(3)
						(28–25–26–27)	0.0	0.6(4)
						(11–25–28–24)	180.0	176.8 (2)
						(26–25–28–24)	0.0	0.3 (3)
						(25–26–27–24)	0.0	−0.7(4)

*Ref. [21]; R, bond lengths (Å); A, angles (°); D, dihedral angles (°).

Correlation between the calculated and the experimental X-ray geometric parameters of bond lengths (a) and bond angles (b) for the DMIA molecule is shown in Figure 4. Bond lengths and bond angles correlation R^2 values are 0.9685 and 0.9676, respectively.

Chemical Shifts

The chemical shifts of the most stable conformation of DMIA, which is labeled as number **1**, were calculated using the Gaussian 03 program package.[22] The calculated ^{1}H NMR chemical shifts for the DMIA molecule together with the corresponding experimental values are shown in Table 3 as values relative to tetramethylsilane. ^{1}H NMR chemical shifts were computed using the gauge-independent atomic orbital (GIAO)/B3LYP/6-311++G(2d,2p) method and conductor-like screening model (COSMO) in DMSO.[23] The ^{1}H NMR spectra for the DMIA molecule in DMSO-d_6 showed a singlet peak at 2.73 ppm for indole C—CH_3, at 2.78 ppm for S—CH_3, and at 3.83 ppm for indole N—CH_3. Corresponding calculated values are 2.93, 2.95, and 3.95 ppm, respectively. Aromatic protons in the indole ring appeared at 7.30 ppm (Calc. 7.80 and 7.83 ppm), 7.53 ppm (Calc. 7.91 ppm), and 8.30 ppm (Calc. 8.93 ppm) as multiplets.

Electronic spectra

The electronic spectra of the most stable conformation of DMIA were also calculated using Gaussian 03. The theoretical and experimental maximum absorption wavelengths are presented in Table 4. The electronic spectra of the DMIA molecule were measured in three organic solvents which are chloroform, methanol, and Dimethylsulfoxide (DMSO) at room temperature. The excitation energies and oscillator strengths for the dye at the optimized geometry in the ground state were obtained in the framework of time-dependent DFT (TD-DFT) calculations with the B3LYP method. For the TD-DFT calculations, the COSMO was used to take care of the solvent effects. Experimentally determined maximum absorption values are 451 nm (in chloroform), 471 nm (in methanol), and 460 nm (in DMSO). The λ_{max} values obtained with B3LYP/6-311++G(2d,2p)

1097461x, 2013, 5, Downloaded from https://onlinelibrary.wiley.com/doi/10.1002/qua.24043 by T.C. Cumhurbaskanligi Kutuphanesi, Wiley Online Library on [20/02/2025]. See the Terms and Conditions (https://onlinelibrary.wiley.com/terms-and-conditions) on Wiley Online Library for rules of use; OA articles are governed by the applicable Creative Commons License

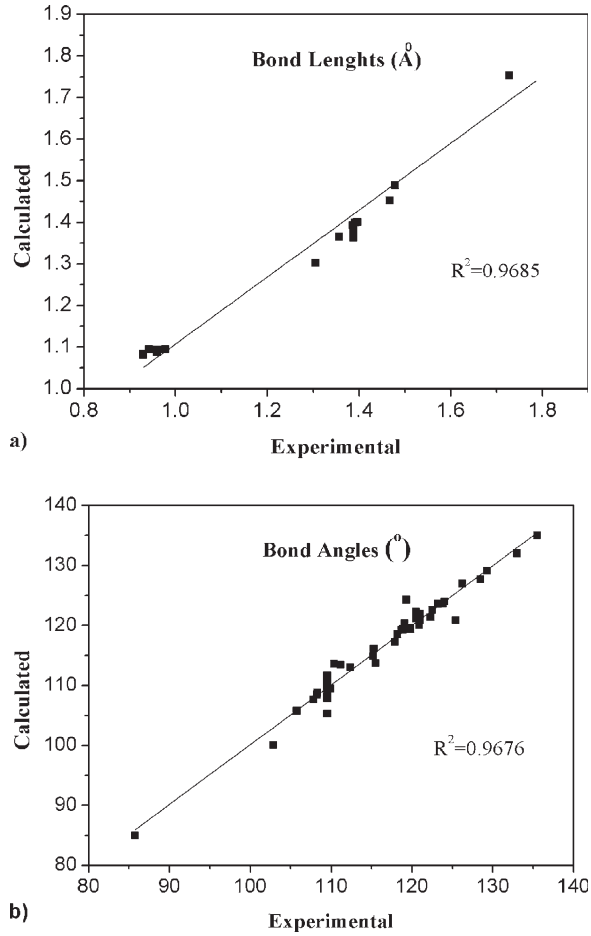


Figure 4. Correlation between the calculated and the experimental*[21] bond lengths a) and bond angles b) for the most stable conformer of the DMIA molecule (**1**).

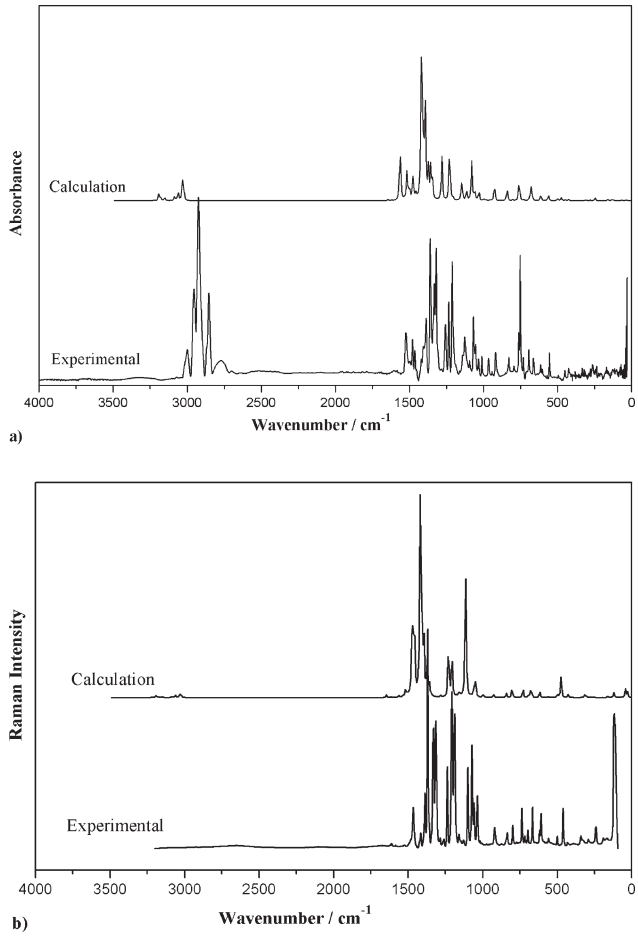


Figure 5. The theoretical and the experimental IR a) and Raman b) spectra of the most stable conformation of the DMIA molecule.

Table 3. Comparison of B3LYP/6–311++G(2d,2p) calculated and experimental values of ^{1}H chemical shifts (ppm) relative to the TMS for the most stable conformation.

	Experimental*		6–311++G(2d,2p)
H15	8.30	(m, 1H, Ar CH)	8.93
H13	7.53	(m, 1H, Ar CH)	7.91
H12	7.30	(m, 2H, Ar CH)	7.83
H14			7.8
H17,H18,H19	3.83	(s, 3H, NCH3)	3.95
H31,H32,H33	2.78	(s, 3H, SCH3)	2.95
H21,H22,H23	2.73	(s, 3H, CCH_3).	2.93

*Ref. [18].

Table 4. The experimental and the calculated absorption maxima for the most stable conformer.

	DMSO	Methanol	Chloroform
Experimental*	460	471	451
6–31+G(d,p)	434 (1.0550)	429 (1.0160)	432 (1.0454)
6–311+G(d,p)	435 (1.0558)	430 (1.0166)	432 (1.0438)
6–311++G(2d,2p)	437 (1.0571)	432 (1.0165)	434 (1.0468)

*Ref. [18], Wavelengths are given in nanometer (nm). The oscillator strength is listed between brackets.

are 434 nm (in chloroform), 432 nm (in methanol), and 437 nm (in DMSO). The values obtained with B3LYP/6-311++G(2d,2p) are much closer to the experimental ones than those with others basis sets. The addition of polarized and diffuse functions to the basis sets cause systematic bathochromic shifts.

Vibrational spectra

The optimized structure and assignment of the fundamental vibrations of the most stable conformation are reported at the B3LYP/6-311+G(d,p) level using Gaussian 03 program. The reason for selecting this computational scheme is that it reproduces experimental frequencies with high accuracy for the aromatic molecules if the calculated force field scaling procedure compensates for the approximations involved in the DFT calculations and for the anharmonicity that is omitted in the usual harmonic approximation.[24–35] The molecular vibrations of the DMIA molecule were investigated by FTIR and FT-Raman spectroscopy. The harmonic and anharmonic vibrational wavenumbers and absolute intensities were calculated by means of the B3LYP/6-311+G(d,p) methods at the corresponding optimized geometry. The calculated and the experimental IR and Raman spectra of DMIA are shown in Figures 5a and 5b.

The calculated harmonic and anharmonic frequencies, experimental FTIR, FT-Raman frequencies, relative IR and Raman

1097461x, 2013, 5, Downloaded from https://onlinelibrary.wiley.com/doi/10.1002/qua.24043 by T.C. Cumhurbaskanligi Kutuphanesi, Wiley Online Library on [20/02/2025]. See the Terms and Conditions (https://onlinelibrary.wiley.com/terms-and-conditions) on Wiley Online Library for rules of use; OA articles are governed by the applicable Creative Commons License

Table 5. The assignments of the fundamental vibrations for the most stable conformation of the DMIA molecule.

		Calculated					Experimental		
Mode no	Symmetry	Har.	Anhar.	I_{IR}	I_R	SQM	IR	R	(%)TED
1	A″	28	75	1.5	1644.0	29	30vs		τ(CNNC)(24) + τ(NNCC)(23) + τ(SCNN)(22)
2	A″	37	38	1.1	85.6	34			τ(CSCS)(18) + τ(NCNN)(17) + τ(CSCN)(14) + τ(CSCN)(14)
3	A′	42	32	1.1	1783.9	41	41m		δ(CNN)(56) + δ(NCC)(17) + δ(SCN)(11)
4	A″	43	726	0.3	771.9	44	46vw		τ(HCNC)(86)
5	A″	68	85	2.4	81.3	66	67vw		τ(CSCS)(34) + τ(CSCN)(26) + τ(NNCC)(10)
6	A″	94	101	0.6	132.8	91	91vw		τ(CSCS)(17) + τ(NCNN)(15)
7	A′	118	115	0.8	1551.6	114			δ(CCN)(27) + δ(NNC)(14) + δ(SCN)(13)
8	A″	126	123	1.5	205.1	119		117s	τ(CCNC)(24) + τ(CCCC)(17)
9	A″	133	137	2.8	191.7	127			τ(CCNC)(34)
10	A″	151	121	0.4	70.3	143			τ(HCSC)(80)
11	A′	159	147	3.7	307.0	154			δ(CSC)(34) + δ(NCS)(19) + δ(SCS)(15)
12	A″	163	179	0.3	176.1	155			τ(HCCN)(47) + τ(HCCC)(45)
13	A″	198	194	0.1	25.7	194		191vw	τ(CNNC)(19) + τ(CSCS)(13) + τ(SCNN)(12)
14	A′	246	251	8.9	80.9	237		240vw	δ(NCC)(23) + δ(CNC)(15) + δ(CCC)(13) + δ(CSC)(11)
15	A″	257	254	0.0	161.6	252			τ(NNCC)(23) + τ(NNCC)(11)
16	A′	280	285	2.0	231.7	270			δ(CNC)(22) + δ(NNC)(12)
17	A′	304	301	2.9	588.1	293		292vw	δ(CNC)(20) + ν(CS)(17) + δ(CSC)(14) + δ(SCS)(13)
18	A″	310	314	0.1	27.4	298			τ(NCCC)(16) + τ(CCCC)(11)
19	A′	317	318	0.8	1007.7	306			δ(CSC)(21) + δ(CCC)(12) + δ(CCN)(10)
20	A″	389	392	0.2	0.9	385			τ(SCNN)(18) + τ(CCNN)(14) + τ(NCNN)(11) + τ(CSCN)(10)
21	A″	425	422	0.5	30.6	410	405vw		ν(CS)(34)
22	A′	427	421	2.9	1025.1	416	415vw		τ(CCCC)(14) + τ(CNNC)(11)
23	A″	447	440	3.0	61.1	431		431vw	τ(NNCC)(10)
24	A′	475	469	11.5	7377.1	456		461w	δ(SCN)ar(16) + ν(CS)(14)
25	A′	499	493	8.0	1143.0	480	496vw	500vw	ν(CC)(13)
26	A′	562	556	19.5	463.3	541			δ(CCN)(20) + δδ(CNC)(16) + ν(CN)(15) + ν(CC)(13)
27	A″	577	568	0.3	9.3	560		560vw	τ(CCCC)(34)
28	A″	585	580	0.2	22.0	577		575vw	τ(CSCN)(38) + τ(NNCS)(29)
29	A″	609	604	0.1	104.9	590			ν(CS)(21) + δ(NCC)(11)
30	A′	613	604	19.2	444.7	594			ν(CS)(37)
31	A′	618	611	2.0	1862.9	606		607w	τ(CNNC)(24) + τ(CSCN)(10)
32	A′	670	663	7.9	1492.2	644			ν(CS)(15) + δ(CCC)(17)
33	A″	677	670	5.5	15.8	653			ν(CS)(27)
34	A′	680	668	44.1	2295.2	654			τ(CNNC)(10)
35	A′	695	676	3.2	674.6	661	660vw	665w	ν(CS)(99)
36	A′	730	722	3.0	3322.0	699	696w	697vw	ν(CS)(18) + ν(CN)(12) + δ(NNC)(11)
37	A″	760	747	70.3	84.7	725			τ(HCCC)(58) + τ(HCCN)(13)
38	A″	778	760	0.5	4.8	744			τ(HCCC)(20) + τ(HCCN)(18) + τ(CCCN)(16)
39	A′	803	794	4.0	3215.5	770			ν(CN)(13)
40	A′	842	833	39.1	1887.0	810		800vw	δ(NNC)(28) + ν(CC)(10)
41	A″	870	850	0.3	20.3	831	830vw	835vw	τ(HCCC)(52) + τ(HCCH)(19) + τ(HCCN)(15)
42	A′	927	918	57.0	1596.5	885			ν(CC)(15) + ν(CN)(15)
43	A″	956	942	1.4	6.1	911			τ(HCCH)(47) + τ(HCCC)(32)
44	A″	983	969	2.9	55.0	943	943vw	920vw	δ(HCS)(88)
45	A′	997	976	6.6	1457.8	954			τ(HCCH)(56) + τ(HCCC)(20)
46	A″	999	974	0.3	1.2	959	968w		δ(HCS)(73) + τ(HCSC)(16)
47	A′	1031	1016	33.3	270.4	984			ν(CC)(48)
48	A′	1048	1033	2.3	6677.0	1003			ν(CC)(14) + δ(HCC)(13)
49	A″	1055	1037	0.6	44.1	1005			δ(HCC)(69) + τ(HCCC)(14)
50	A′	1060	1041	31.9	3823.4	1017	1013w	1018vw	ν(CS)(32) + ν(NN)ar(20) + δ(CNN)(21) + δ(NCS)(16)
51	A′	1079	1063	142.6	459.8	1035	1035w	1036m	ν(CN)(20) + δ(HCC)ar(22)
52	A′	1115	1088	34.7	55013.6	1068	1067m	1071s	ν(NN)(56) + δ(NCS)(12)
53	A″	1141	1131	0.1	7.4	1087	1086vw		δ(HCN)(74) + τ(HCNC)(16)
54	A′	1146	1132	66.9	369.5	1093	1094vw	1099m	δ(HCC)ar(23) + ν(CC)(18) + δ(HCN)(14)
55	A′	1159	1145	5.6	2201.0	1105			δ(HCC)ar(16) + ν(NN)(11)
56	A′	1176	1161	0.3	534.2	1121	1126w		δ(HCC)ar(58)
57	A′	1207	1185	10.6	18501.5	1151			ν(CC)ar(43)
58	A′	1229	1200	192.5	21990.1	1176	1161vw	1186s	ν(CN)(52)
59	A′	1281	1262	141.6	594.8	1223	1212m	1206s	δ(HCC)ar(35) + ν (CN)(14) + ν(CC)ar(13)
60	A′	1346	1317	81.6	562.5	1287	1290vw		δ(HCC)ar(28) + ν(CC)ar(21)
61	A′	1358	1322	100.2	4458.7	1309	1309w		ν(CC)ar(59)
62	A′	1373	1345	105.9	13630.4	1315	1320vs	1315s	ν(CN)ar(38) + δ(HCS)(21) + δ(HCH)(16)
63	A′	1395	1359	347.0	24350.9	1340	1341m	1330s	ν(CN)ar(29) + δ(HCS)(26) + δ(HCH)(24)
64	A′	1406	1380	117.4	20059.1	1347		1346vw	ν(CN)(40)

(Continued)

1097461x, 2013, 5, Downloaded from https://onlinelibrary.wiley.com/doi/10.1002/qua.24043 by T.C. Cumhurbaskanligi Kutuphanesi, Wiley Online Library on [20/02/2025]. See the Terms and Conditions (https://onlinelibrary.wiley.com/terms-and-conditions) on Wiley Online Library for rules of use; OA articles are governed by the applicable Creative Commons License

Table 5 (*Continued*)

Mode no	Symmetry	Calculated Har.	Anhar.	I_{IR}	I_R	SQM	Experimental IR	R	(%)TED
65	A′	1414	1384	55.4	2690.0	1356	1360vs		ν(CN)(29) + ν(NN)(23)
66	A′	1418	1384	602.3	108397.6	1376		1368vs	δ(HCC)(45) + δ(HCH)(43)
67	A″	1455	1410	11.3	265.0	1409	1408w		ν(NN)(14)
68	A′	1458	1437	9.6	27043.4	1413		1415vw	δ(HCC)ar(18) + ν(CC)ar(15) + ν(CN)(10)
69	A′	1468	1440	6.5	26457.0	1429	1420vw	1425vw	δ(HCH)(31)
70	A′	1476	1439	49.7	5280.4	1437			δ(HCC)ar(23) + ν(CC)ar(14)
71	A′	1477	1448	12.9	14402.5	1449			δ(HCH)(70) + τ(HCSC)(16)
72	A″	1481	1466	16.6	192.1	1450			ν(CN)(24) + ν(NN)(12)
73	A″	1496	1471	0.0	86.3	1451			δ(HCH)(58)
74	A′	1498	1474	24.7	250.6	1458	1452vw		δ(HCH)(31)
75	A′	1507	1479	25.0	852.4	1466			δ(HCH) + τ(HCSC)
76	A′	1518	1482	99.7	2734.5	1468	1465w	1465w	δ(HCH)(69) + τ(HCSC)(22)
77	A′	1536	1502	5.6	506.7	1490	1481w	1483vw	δ(HCH)(37) + δ(HCC)ar(16)
78	A′	1563	1530	185.6	870.2	1500	1500vw		ν(CC)ar(33) + δ(HCC)(14)
79	A′	1618	1579	1.4	332.2	1545			ν(CC)ar(60)
80	A′	1646	1607	3.5	1358.0	1572		1584vw	ν(CC)ar(61)
81	A′	3022	2917	30.5	1699.0	2905			$\nu(CH_3)$s(100)
82	A′	3033	2917	72.7	2157.8	2916			$\nu(CH_3)$s(99)
83	A′	3060	2944	22.5	1294.6	2941			$\nu(CH_3)$s(91)
84	A″	3068	2926	10.1	512.1	2949	2923vs		$\nu(CH_3)$as(100)
85	A″	3085	2942	14.7	637.7	2966	2955s		$\nu(CH_3)$as(100)
86	A′	3141	2999	1.5	84.3	3020			$\nu(CH_3)$as(91)
87	A′	3151	3006	2.9	463.4	3029			$\nu(CH_3)$as(99)
88	A′	3152	3005	5.0	220.8	3031			$\nu(CH_3)$as(90)
89	A″	3159	3011	2.3	228.6	3036			$\nu(CH_3)$as(100)
90	A′	3169	3025	0.6	194.5	3046	3026vw		ν(CH)ar(99)
91	A′	3181	3050	13.0	505.2	3058			ν(CH)ar(96)
92	A′	3192	3063	20.6	1255.5	3068	3072vw		ν(CH)ar(98)
93	A′	3224	3080	1.8	143.3	3099			ν(CH)ar(97)

Har: harmonic frequencies (cm^{-1}); Anhar: anharmonic frequencies (cm^{-1}); IIR: Relative Infrared intensities; IR: Relative Raman intensities; SQM: Scaled Quantum Mechanic Calculation; TED less than %10 are not shown; ν, stretching; δ, bending; ⊤, torsion; ar, aromatic; s, symmetric; as, asymmetric; vw, very weak; s, strong; m, medium; w, weak; vs, very strong.

intensities and total energy distribution (TED) of the fundamental vibrational bands of the studied molecule are given in Table 5. The theoretical Raman intensities (I_R) can be obtained from the computed Raman scattering activities using the following equations:

$$I_R = C(\upsilon_0 - \upsilon_i)^4 .\ \upsilon_i^{-1} .\ B_i^{-1} .S_i,$$

where B_i is a temperature factor, which accounts for the intensity contribution of excited vibrational states and is represented by the Boltzmann distribution and υ_0 is the wavenumber of the laser excitation line. In this work, 13,605.44 cm^{-1} was used as excitation wavenumber, which corresponds to the wavelength of 735 nm. S_i is the Raman scattering activity of the normal mode[36] and $C = 10^{-12}$ is a constant.

The DMIA molecule belongs to Cs point group and its 93 normal vibration modes will span the irreducible representation that is, 60A′ (in plane) + 33A″ (out of plane). For the calculation of vibration frequencies, a scaling factor of 0.9613 has been used. Generally, a systematic error between the calculated and the experimental spectra occurs because of neglecting anharmonic effects, electron correlation and basis set defects. Scaling of calculated vibrational spectra is very useful as it accounts for systematic errors.[37,38]

The characteristic C—H stretching vibrations of heteroaromatic structure are expected to appear in the wavenumber range 3000–3100 cm^{-1}.[39] The bands observed at 3072 and 3026 cm^{-1} in IR spectrum of the DMIA molecule are identified as aromatic CH stretching vibrations. CH_3 asymmetric stretching vibrations are assigned at 2923 and 2955 cm^{-1}. The calculated wavenumbers are 2949 and 2966 cm^{-1}, respectively.

The observed bands in the region 1320–1481 cm^{-1} in the IR spectrum and 1315–1465 cm^{-1} in the Raman spectrum are assigned to HCH bending vibrations. HCS out of plane bending vibrations were observed at 943 cm^{-1} (IR), 920 cm^{-1} (R), and 968 cm^{-1} (IR). Two peaks at 1320 and 1341 cm^{-1} in the IR spectrum and two peaks at 1315 and 1330 cm^{-1} in the Raman spectrum are assigned to the HCS in plane bending vibrations. The theoretically calculated HCS in plane bending vibrations (1315 and 1340 cm^{-1}) are in good agreement with the experimental values. The observed bands in the region 1035–1500 cm^{-1} in the IR spectrum are assigned to HCC in plane bending vibrations.

C=N, C=C, and N=N stretching vibrations are predicted in the region 1500–1212 cm^{-1} (IR). N=N stretching vibrations are expressed in a weak band at 1408 cm^{-1} and a very strong band at 1360 cm^{-1} in the IR spectrum. The N—N stretching of the thiadiazole ring is assigned to the experimental bands at 1067 cm^{-1} (IR), 1071 cm^{-1} (R) and 1013 cm^{-1} (IR), 1018 cm^{-1} (R).

1097461x, 2013, 5, Downloaded from https://onlinelibrary.wiley.com/doi/10.1002/qua.24043 by T.C. Cumhurbaskanligi Kutuphanesi, Wiley Online Library on [20/02/2025]. See the Terms and Conditions (https://onlinelibrary.wiley.com/terms-and-conditions) on Wiley Online Library for rules of use; OA articles are governed by the applicable Creative Commons License

The S—CH_3 stretching mode is assigned to a very weak IR band at 660 cm^{-1} (IR) and a weak band at 665 cm^{-1}. The theoretically computed value at 661 cm^{-1} exactly coincides with the experimental results. The C—S—CH_3 angle of the bending mode is assigned at 240 cm^{-1} and 292 cm^{-1} in Raman spectra. The N—CH_3 stretching frequencies are established at 1360, 1035, and 696 cm^{-1} in the IR spectrum and at 1036 and 697 cm^{-1} in the Raman spectra.

The complete assignments were performed on the basis of the TED of the vibrational modes, calculated with scaled quantum mechanics (SQM) method, using the SQM program.[40] The calculated root mean square (RMS) value, obtained using the SQM method is 4.77 cm^{-1}.

Conclusions

The DMIA was studied by means of FTIR, FT-Raman, and NMR spectra and by DFT calculations. All observed vibrational bands have been examined and assigned with the help of TED values obtained by our calculations. The results from the experimental and the theoretical methods indicate that the density functional methods provide valuable information for understanding the vibrational spectra of the DMIA molecule.

Acknowledgements

The authors thank the Central Laboratory of Anadolu University for recording the IR and Raman spectra of the sample.

Keywords: hetarylazo indole dye · DFT · vibrational frequencies · SQM · TD-DFT · GIAO

How to cite this article: B. Çatıkkaş, E. Aktan, Z. Seferoğlu, *Int. J. Quantum Chem.* **2013,** *113,* 683–689. DOI: 10.1002/qua.24043

[1] K. Hunger, *Industrial Dyes, Chemistry, Properties, Applications*; Wiley-VCH Verlag GmbH KgaA: Weinheim, **2003**, pp. 20–35.
[2] S. C. Catino, R. E. Farris, In *Concise Encyclopedia of Chemical Technology.*; M. Grayson Ed; Wiley: New York, **1985**, p. 142.
[3] H. Zollinger, *Color Chemistry: Synthesis, Properties and Applications of Organic Dyes and Pigments*, 3rd ed.; Wiley-VCH: Weinheim, **2003**.
[4] F. N. Karcı, *Ertan Dyes Pigments* **2005**, *64,* 243.
[5] K. Tanaka, K. Matsuo, A. Nakanishi, J. H. Shiota, M. Yamaguchi, S. Yoshino, *Chem. Pharm. Bull.* **1984**, *32,* 391.
[6] A. A. Fadda, H. A. Etmen, F. A. Amer, M. Barghout, K. S. Mohammed, *J. Chem. Technol. Biotechnol.* **1994**, *61,* 343.
[7] J. Isaad, A. Perwuelz, *Tetrahedron Lett.* **2010**, *51,* 5810.
[8] Q. Wang, Y. Long, L. Liangliang, Z. Chuanzheng, X. Zhen, *Tetrahedron Lett.* **2008**, *49,* 5087.
[9] J. Wang, C. S. Ha, *Tetrahedron* **2009**, *65,* 6959.
[10] H. Bach, K. Anderle, Th. Fuhrmann, J. H. Wendorff, *J. Phys. Chem.* **1996**, *100,* 4135.
[11] R. J. H. Clark, R. E. Hester, *Spectroscopy of New Materials Advances in Spectroscopy*; Wiley: New York. **1993**.
[12] K. Taniike, T. Matsumoto, T. Sato, Y. Ozaki, K. Nakashima, K. Iriyama, *J. Phys. Chem.* **1996**, *100,* 15508.
[13] N. Biswas, S. Umapathy, *J. Phys. Chem. A* **2000**, *104,* 2734.
[14] I. Willner, S. Rubin, *Angew. Chem. Int. Ed. Engl.* **1996**, *35,* 367.
[15] (a) Z. Seferoğlu, T. Hökelek, E. Sahin, N. Ertan, *Acta Crystallogr.* **2006**, *E62,* o2108–o2110; (b) Z. Seferoğlu, T. Hökelek, E. Sahin, N. Ertan, *Acta Crystallogr.* **2006**, *E62,* o3492–o3494; (c) Z. Seferoğlu, T. Hökelek, E. Sahin, N. Ertan, *Acta Crystallogr.* **2006**, *E62,* o3835–o3837.
[16] Z. Seferoğlu, T. Hökelek, E. Sahin, A. Saylam, N. Ertan, *Acta Crystallogr.* **2006**, *E62,* o5488–o5489.
[17] (a) Z. Seferoğlu, T. Hökelek, E. Sahin, N. Ertan, *Acta Crystallogr.* **2007**, *E63,* o148–o150; (b) Z. Seferoğlu, T. Hökelek, E. Sahin, N. Ertan, *Acta Crystallogr.* **2007**, *E63,* o351–o353; (c) Z. Seferoğlu, T. Hökelek, E. Sahin, N. Ertan, *Acta Crystallogr.* **2007**, *E63,* o568–o570.
[18] Z. Seferoğlu, N. Ertan, T. Hokelek, E. Şahin, *Dyes Pigments* **2008**, *77,* 614.
[19] C. Lee, W. Yang, R. G. Parr, *Phys. Rev. B* **1998**, *37,* 785.
[20] J. B. Foresman, E. Frisch, Exploring Chemistry with Electronic Structure Methods, Vol. *118; Gaussian: Pittsburgh, PA,* **1996**.
[21] Z. Seferoğlu, T. Hökelek, E. Sahin, N. Ertan, *Acta Crystallogr.* **2007**, *E63,* o2263–o2264.
[22] Gaussian 03, Revision D.01, Gaussian, Wallingford CT, **2004**.
[23] V. Barone, M. Cossi, *J. Phys. Chem. A* **1998**, *102,* 1995.
[24] R. N. Brogden, *Drugs,* **1986**, *32,* 60.
[25] K. L. Kees, J. J. Fitzgerald, K. E. Steiner, J. F. Mattes, B. Mihan, T. Tosi, D. Mondoro, M. C. Mc Caleb, *J. Med. Chem.* **1996**, *39,* 3920.
[26] P. Pulay, G. Fogarasi, G. Pongor, J. E. Boggs, A. Vargha, *J. Am. Chem. Soc.* **1983**, *105,* 7037.
[27] G. Rauhut, P. Pulay, *J. Phys. Chem.* **1995**, *99,* 3096.
[28] J. Baker, A. A. Jarzecki, P. Pulay, *J. Phys. Chem. A* **1998**, *102,* 1412.
[29] K. Koch, M. C. Holthausen, *A Chemist's Guide to Density Functional Theory*; Wiley-VCH: Weinheim, **2001**, p. 251.
[30] N. C. Hardy, P. E. Maslen, R. D. Amos, J. S. Andrews, C. W. Murray, G. Laming, *J. Chem. Phys. Lett.* **1992**, *197,* 50.
[31] P. J. Stephens, F. J. Devlin, C. F. Chabalowshi, M. J. Frisch, *J. Phys. Chem.* **1994**, *98,* 11623.
[32] A. A. El-Azhary, H. U. Suter, *J. Phys. Chem.* **1995**, *99,* 12751.
[33] S. Y. Lee, B. H. Boo, *Bull. Korean Chem. Soc.* **1996**, *17,* 760.
[34] S. Y. Lee, *Bull. Korean Chem. Soc.* **2001**, *22,* 605.
[35] T. Sundius, *Vib. Spectrosc.* **2002**, *29,* 89.
[36] D. Michalska, R. Wysokiński, *Chem. Phys. Lett.* **2005**, *403,* 211.
[37] Y. Yamaguchi, M. Frisch, J. Gaw, H. F. Schaefer, J. S. Binkley, *J. Chem. Phys.* **1986**, *84,* 2262.
[38] P. Pulay, G. Fogarasi, F. F. Pang, J. E. Boggs, *J. Am. Chem. Soc.* **1979**, *101,* 2550.
[39] G. Varsanyi, Vibrational Spectra of Benzene Derivatives; Academic Press: New York, **1969**.
[40] SQM version 1.0, Parallel Quantum Solutions, Fayetteville, AR, **2009**.

Received: 1 November 2011
Revised: 23 December 2011
Accepted: 29 December 2011
Published online on 6 March 2012

1097461x, 2013, 5, Downloaded from https://onlinelibrary.wiley.com/doi/10.1002/qua.24043 by T.C. Cumhurbaskanligi Kutliyesi, Wiley Online Library on [20/02/2025]. See the Terms and Conditions (https://onlinelibrary.wiley.com/terms-and-conditions) on Wiley Online Library for rules of use; OA articles are governed by the applicable Creative Commons License